

UC Berkeley

UC Berkeley Previously Published Works

Title

Improved limits on the lepton-flavor violating decays $\tau \rightarrow \ell^+ \ell^-$.

Permalink

<https://escholarship.org/uc/item/6jf5p8t3>

Journal

Physical review letters, 99(25)

ISSN

0031-9007

Authors

Aubert, B
Bona, M
Boutigny, D
[et al.](#)

Publication Date

2007-12-19

DOI

10.1103/physrevlett.99.251803

License

<https://creativecommons.org/licenses/by/4.0/> 4.0

Peer reviewed

Improved Limits on the Lepton-Flavor Violating Decays $\tau^- \rightarrow l^- l^+ l^-$

B. Aubert,¹ M. Bona,¹ D. Boutigny,¹ Y. Karyotakis,¹ J. P. Lees,¹ V. Poireau,¹ X. Prudent,¹ V. Tisserand,¹ A. Zghiche,¹ J. Garra Tico,² E. Grauges,² L. Lopez,³ A. Palano,³ M. Pappagallo,³ G. Eigen,⁴ B. Stugu,⁴ L. Sun,⁴ G. S. Abrams,⁵ M. Battaglia,⁵ D. N. Brown,⁵ J. Button-Shafer,⁵ R. N. Cahn,⁵ Y. Groysman,⁵ R. G. Jacobsen,⁵ J. A. Kadyk,⁵ L. T. Kerth,⁵ Yu. G. Kolomensky,⁵ G. Kukartsev,⁵ D. Lopes Pegna,⁵ G. Lynch,⁵ L. M. Mir,⁵ T. J. Orimoto,⁵ I. L. Osipenkov,⁵ M. T. Ronan,^{5,*} K. Tackmann,⁵ T. Tanabe,⁵ W. A. Wenzel,⁵ P. del Amo Sanchez,⁶ C. M. Hawkes,⁶ A. T. Watson,⁶ H. Koch,⁷ T. Schroeder,⁷ D. Walker,⁸ D. J. Asgeirsson,⁹ T. Cuhadar-Donszelmann,⁹ B. G. Fulsom,⁹ C. Hearty,⁹ T. S. Mattison,⁹ J. A. McKenna,⁹ M. Barrett,¹⁰ A. Khan,¹⁰ M. Saleem,¹⁰ L. Teodorescu,¹⁰ V. E. Blinov,¹¹ A. D. Bukin,¹¹ V. P. Druzhinin,¹¹ V. B. Golubev,¹¹ A. P. Onuchin,¹¹ S. I. Serednyakov,¹¹ Yu. I. Skovpen,¹¹ E. P. Solodov,¹¹ K. Yu. Todyshev,¹¹ M. Bondioli,¹² S. Curry,¹² I. Eschrich,¹² D. Kirkby,¹² A. J. Lankford,¹² P. Lund,¹² M. Mandelkern,¹² E. C. Martin,¹² D. P. Stoker,¹² S. Abachi,¹³ C. Buchanan,¹³ S. D. Foulkes,¹⁴ J. W. Gary,¹⁴ F. Liu,¹⁴ O. Long,¹⁴ B. C. Shen,¹⁴ G. M. Vitug,¹⁴ L. Zhang,¹⁴ H. P. Paar,¹⁵ S. Rahatlou,¹⁵ V. Sharma,¹⁵ J. W. Berryhill,¹⁶ C. Campagnari,¹⁶ A. Cunha,¹⁶ B. Dahmes,¹⁶ T. M. Hong,¹⁶ D. Kovalskyi,¹⁶ J. D. Richman,¹⁶ T. W. Beck,¹⁷ A. M. Eisner,¹⁷ C. J. Flacco,¹⁷ C. A. Heusch,¹⁷ J. Kroseberg,¹⁷ W. S. Lockman,¹⁷ T. Schalk,¹⁷ B. A. Schumm,¹⁷ A. Seiden,¹⁷ M. G. Wilson,¹⁷ L. O. Winstrom,¹⁷ E. Chen,¹⁸ C. H. Cheng,¹⁸ F. Fang,¹⁸ D. G. Hitlin,¹⁸ I. Narsky,¹⁸ T. Piatenko,¹⁸ F. C. Porter,¹⁸ R. Andreassen,¹⁹ G. Mancinelli,¹⁹ B. T. Meadows,¹⁹ K. Mishra,¹⁹ M. D. Sokoloff,¹⁹ F. Blanc,²⁰ P. C. Bloom,²⁰ S. Chen,²⁰ W. T. Ford,²⁰ J. F. Hirschauer,²⁰ A. Kreisel,²⁰ M. Nagel,²⁰ U. Nauenberg,²⁰ A. Olivas,²⁰ J. G. Smith,²⁰ K. A. Ulmer,²⁰ S. R. Wagner,²⁰ J. Zhang,²⁰ A. M. Gabareen,²¹ A. Soffer,^{21,†} W. H. Toki,²¹ R. J. Wilson,²¹ F. Winklmeier,²¹ D. D. Altenburg,²² E. Feltresi,²² A. Hauke,²² H. Jasper,²² J. Merkel,²² A. Petzold,²² B. Spaan,²² K. Wacker,²² V. Klose,²³ M. J. Kobel,²³ H. M. Lacker,²³ W. F. Mader,²³ R. Nogowski,²³ J. Schubert,²³ K. R. Schubert,²³ R. Schwierz,²³ J. E. Sundermann,²³ A. Volk,²³ D. Bernard,²⁴ G. R. Bonneaud,²⁴ E. Latour,²⁴ V. Lombardo,²⁴ Ch. Thiebaut,²⁴ M. Verderi,²⁴ P. J. Clark,²⁵ W. Gradl,²⁵ F. Muheim,²⁵ S. Playfer,²⁵ A. I. Robertson,²⁵ J. E. Watson,²⁵ Y. Xie,²⁵ M. Andreotti,²⁶ D. Bettoni,²⁶ C. Bozzi,²⁶ R. Calabrese,²⁶ A. Cecchi,²⁶ G. Cibinetto,²⁶ P. Franchini,²⁶ E. Luppi,²⁶ M. Negrini,²⁶ A. Petrella,²⁶ L. Piemontese,²⁶ E. Prencipe,²⁶ V. Santoro,²⁶ F. Anulli,²⁷ R. Baldini-Ferrolì,²⁷ A. Calcaterra,²⁷ R. de Sangro,²⁷ G. Finocchiaro,²⁷ S. Pacetti,²⁷ P. Patteri,²⁷ I. M. Peruzzi,^{27,‡} M. Piccolo,²⁷ M. Rama,²⁷ A. Zallo,²⁷ A. Buzzo,²⁸ R. Contri,²⁸ M. Lo Vetere,²⁸ M. M. Macri,²⁸ M. R. Monge,²⁸ S. Passaggio,²⁸ C. Patrignani,²⁸ E. Robutti,²⁸ A. Santroni,²⁸ S. Tosi,²⁸ K. S. Chaisanguanthum,²⁹ M. Morii,²⁹ J. Wu,²⁹ R. S. Dubitzky,³⁰ J. Marks,³⁰ S. Schenk,³⁰ U. Uwer,³⁰ D. J. Bard,³¹ P. D. Dauncey,³¹ R. L. Flack,³¹ J. A. Nash,³¹ W. Panduro Vazquez,³¹ M. Tibbetts,³¹ P. K. Behera,³² X. Chai,³² M. J. Charles,³² U. Mallik,³² J. Cochran,³³ H. B. Crawley,³³ L. Dong,³³ V. Eyges,³³ W. T. Meyer,³³ S. Prell,³³ E. I. Rosenberg,³³ A. E. Rubin,³³ Y. Y. Gao,³⁴ A. V. Gritsan,³⁴ Z. J. Guo,³⁴ C. K. Lae,³⁴ A. G. Denig,³⁵ M. Fritsch,³⁵ G. Schott,³⁵ N. Arnaud,³⁶ J. Béguilleux,³⁶ A. D'Orazio,³⁶ M. Davier,³⁶ G. Grosdidier,³⁶ A. Höcker,³⁶ V. Lepeltier,³⁶ F. Le Diberder,³⁶ A. M. Lutz,³⁶ S. Pruvot,³⁶ S. Rodier,³⁶ P. Roudeau,³⁶ M. H. Schune,³⁶ J. Serrano,³⁶ V. Sordini,³⁶ A. Stocchi,³⁶ W. F. Wang,³⁶ G. Wormser,³⁶ D. J. Lange,³⁷ D. M. Wright,³⁷ I. Bingham,³⁸ J. P. Burke,³⁸ C. A. Chavez,³⁸ J. R. Fry,³⁸ E. Gabathuler,³⁸ R. Gamet,³⁸ D. E. Hutchcroft,³⁸ D. J. Payne,³⁸ K. C. Schofield,³⁸ C. Touramanis,³⁸ A. J. Bevan,³⁹ K. A. George,³⁹ F. Di Lodovico,³⁹ R. Sacco,³⁹ G. Cowan,⁴⁰ H. U. Flaecher,⁴⁰ D. A. Hopkins,⁴⁰ S. Paramesvaran,⁴⁰ F. Salvatore,⁴⁰ A. C. Wren,⁴⁰ D. N. Brown,⁴¹ C. L. Davis,⁴¹ J. Allison,⁴² D. Bailey,⁴² N. R. Barlow,⁴² R. J. Barlow,⁴² Y. M. Chia,⁴² C. L. Edgar,⁴² G. D. Lafferty,⁴² T. J. West,⁴² J. I. Yi,⁴² J. Anderson,⁴³ C. Chen,⁴³ A. Jawahery,⁴³ D. A. Roberts,⁴³ G. Simi,⁴³ J. M. Tuggle,⁴³ G. Blaylock,⁴⁴ C. Dallapiccola,⁴⁴ S. S. Hertzbach,⁴⁴ X. Li,⁴⁴ T. B. Moore,⁴⁴ E. Salvati,⁴⁴ S. Saremi,⁴⁴ R. Cowan,⁴⁵ D. Dujmic,⁴⁵ P. H. Fisher,⁴⁵ K. Koeneke,⁴⁵ G. Sciolla,⁴⁵ M. Spitznagel,⁴⁵ F. Taylor,⁴⁵ R. K. Yamamoto,⁴⁵ M. Zhao,⁴⁵ Y. Zheng,⁴⁵ S. E. Mclachlin,^{46,*} P. M. Patel,⁴⁶ S. H. Robertson,⁴⁶ A. Lazzaro,⁴⁷ F. Palombo,⁴⁷ J. M. Bauer,⁴⁸ L. Cremaldi,⁴⁸ V. Eschenburg,⁴⁸ R. Godang,⁴⁸ R. Kroeger,⁴⁸ D. A. Sanders,⁴⁸ D. J. Summers,⁴⁸ H. W. Zhao,⁴⁸ S. Brunet,⁴⁹ D. Côté,⁴⁹ M. Simard,⁴⁹ P. Taras,⁴⁹ F. B. Viaud,⁴⁹ H. Nicholson,⁵⁰ G. De Nardo,⁵¹ F. Fabozzi,^{51,§} L. Lista,⁵¹ D. Monorchio,⁵¹ C. Sciacca,⁵¹ M. A. Baak,⁵² G. Raven,⁵² H. L. Snoek,⁵² C. P. Jessop,⁵³ K. J. Knoepfel,⁵³ J. M. LoSecco,⁵³ G. Benelli,⁵⁴ L. A. Corwin,⁵⁴ K. Honscheid,⁵⁴ H. Kagan,⁵⁴ R. Kass,⁵⁴ J. P. Morris,⁵⁴ A. M. Rahimi,⁵⁴ J. J. Regensburger,⁵⁴ S. J. Sekula,⁵⁴ Q. K. Wong,⁵⁴ N. L. Blount,⁵⁵ J. Brau,⁵⁵ R. Frey,⁵⁵ O. Igonkina,⁵⁵ J. A. Kolb,⁵⁵ M. Lu,⁵⁵ R. Rahmat,⁵⁵ N. B. Sinev,⁵⁵ D. Strom,⁵⁵ J. Strube,⁵⁵ E. Torrence,⁵⁵ N. Gagliardi,⁵⁶ A. Gaz,⁵⁶ M. Margoni,⁵⁶ M. Morandin,⁵⁶ A. Pompili,⁵⁶ M. Posocco,⁵⁶ M. Rotondo,⁵⁶ F. Simonetto,⁵⁶ R. Stroili,⁵⁶ C. Voci,⁵⁶ E. Ben-Haim,⁵⁷ H. Briand,⁵⁷ G. Calderini,⁵⁷ J. Chauveau,⁵⁷ P. David,⁵⁷ L. Del Buono,⁵⁷ Ch. de la Vaissière,⁵⁷ O. Hamon,⁵⁷ Ph. Leruste,⁵⁷ J. Malcès,⁵⁷ J. Ocariz,⁵⁷ A. Perez,⁵⁷ J. Prendki,⁵⁷ L. Gladney,⁵⁸ M. Biasini,⁵⁹ R. Covarelli,⁵⁹ E. Manoni,⁵⁹ C. Angelini,⁶⁰ G. Batignani,⁶⁰

S. Bettarini,⁶⁰ M. Carpinelli,⁶⁰ R. Cenci,⁶⁰ A. Cervelli,⁶⁰ F. Forti,⁶⁰ M. A. Giorgi,⁶⁰ A. Lusiani,⁶⁰ G. Marchiori,⁶⁰ M. A. Mazur,⁶⁰ M. Morganti,⁶⁰ N. Neri,⁶⁰ E. Paoloni,⁶⁰ G. Rizzo,⁶⁰ J. J. Walsh,⁶⁰ J. Biesiada,⁶¹ P. Elmer,⁶¹ Y. P. Lau,⁶¹ C. Lu,⁶¹ J. Olsen,⁶¹ A. J. S. Smith,⁶¹ A. V. Telnov,⁶¹ E. Baracchini,⁶² F. Bellini,⁶² G. Cavoto,⁶² D. del Re,⁶² E. Di Marco,⁶² R. Faccini,⁶² F. Ferrarotto,⁶² F. Ferroni,⁶² M. Gaspero,⁶² P. D. Jackson,⁶² L. Li Gioi,⁶² M. A. Mazzoni,⁶² S. Morganti,⁶² G. Piredda,⁶² F. Polci,⁶² F. Renga,⁶² C. Voena,⁶² M. Ebert,⁶³ T. Hartmann,⁶³ H. Schröder,⁶³ R. Waldi,⁶³ T. Adye,⁶⁴ G. Castelli,⁶⁴ B. Franek,⁶⁴ E. O. Olaiya,⁶⁴ W. Roethel,⁶⁴ F. F. Wilson,⁶⁴ S. Emery,⁶⁵ M. Escalier,⁶⁵ A. Gaidot,⁶⁵ S. F. Ganzhur,⁶⁵ G. Hamel de Monchenault,⁶⁵ W. Kozanecki,⁶⁵ G. Vasseur,⁶⁵ Ch. Yèche,⁶⁵ M. Zito,⁶⁵ X. R. Chen,⁶⁶ H. Liu,⁶⁶ W. Park,⁶⁶ M. V. Purohit,⁶⁶ R. M. White,⁶⁶ J. R. Wilson,⁶⁶ M. T. Allen,⁶⁷ D. Aston,⁶⁷ R. Bartoldus,⁶⁷ P. Bechtel,⁶⁷ R. Claus,⁶⁷ J. P. Coleman,⁶⁷ M. R. Convery,⁶⁷ J. C. Dingfelder,⁶⁷ J. Dorfan,⁶⁷ G. P. Dubois-Felsmann,⁶⁷ W. Dunwoodie,⁶⁷ R. C. Field,⁶⁷ T. Glanzman,⁶⁷ S. J. Gowdy,⁶⁷ M. T. Graham,⁶⁷ P. Grenier,⁶⁷ C. Hast,⁶⁷ W. R. Innes,⁶⁷ J. Kaminski,⁶⁷ M. H. Kelsey,⁶⁷ H. Kim,⁶⁷ P. Kim,⁶⁷ M. L. Kocian,⁶⁷ D. W. G. S. Leith,⁶⁷ S. Li,⁶⁷ S. Luitz,⁶⁷ V. Luth,⁶⁷ H. L. Lynch,⁶⁷ D. B. MacFarlane,⁶⁷ H. Marsiske,⁶⁷ R. Messner,⁶⁷ D. R. Muller,⁶⁷ C. P. O'Grady,⁶⁷ I. Ofte,⁶⁷ A. Perazzo,⁶⁷ M. Perl,⁶⁷ T. Pulliam,⁶⁷ B. N. Ratcliff,⁶⁷ A. Roodman,⁶⁷ A. A. Salnikov,⁶⁷ R. H. Schindler,⁶⁷ J. Schwiening,⁶⁷ A. Snyder,⁶⁷ D. Su,⁶⁷ M. K. Sullivan,⁶⁷ K. Suzuki,⁶⁷ S. K. Swain,⁶⁷ J. M. Thompson,⁶⁷ J. Va'vra,⁶⁷ A. P. Wagner,⁶⁷ M. Weaver,⁶⁷ W. J. Wisniewski,⁶⁷ M. Wittgen,⁶⁷ D. H. Wright,⁶⁷ A. K. Yarritu,⁶⁷ K. Yi,⁶⁷ C. C. Young,⁶⁷ V. Ziegler,⁶⁷ P. R. Burchat,⁶⁸ A. J. Edwards,⁶⁸ S. A. Majewski,⁶⁸ T. S. Miyashita,⁶⁸ B. A. Petersen,⁶⁸ L. Wilden,⁶⁸ S. Ahmed,⁶⁹ M. S. Alam,⁶⁹ R. Bula,⁶⁹ J. A. Ernst,⁶⁹ V. Jain,⁶⁹ B. Pan,⁶⁹ M. A. Saeed,⁶⁹ F. R. Wappler,⁶⁹ S. B. Zain,⁶⁹ M. Krishnamurthy,⁷⁰ S. M. Spanier,⁷⁰ R. Eckmann,⁷¹ J. L. Ritchie,⁷¹ A. M. Ruland,⁷¹ C. J. Schilling,⁷¹ R. F. Schwitters,⁷¹ J. M. Izen,⁷² X. C. Lou,⁷² S. Ye,⁷² F. Bianchi,⁷³ F. Gallo,⁷³ D. Gamba,⁷³ M. Pelliccioni,⁷³ M. Bomben,⁷⁴ L. Bosisio,⁷⁴ C. Cartaro,⁷⁴ F. Cossutti,⁷⁴ G. Della Ricca,⁷⁴ L. Lanceri,⁷⁴ L. Vitale,⁷⁴ V. Azzolini,⁷⁵ N. Lopez-March,⁷⁵ F. Martinez-Vidal,⁷⁵ D. A. Milanes,⁷⁵ A. Oyanguren,⁷⁵ J. Albert,⁷⁶ Sw. Banerjee,⁷⁶ B. Bhuyan,⁷⁶ K. Hamano,⁷⁶ R. Kowalewski,⁷⁶ I. M. Nugent,⁷⁶ J. M. Roney,⁷⁶ R. J. Sobie,⁷⁶ P. F. Harrison,⁷⁷ J. Ilic,⁷⁷ T. E. Latham,⁷⁷ G. B. Mohanty,⁷⁷ H. R. Band,⁷⁸ X. Chen,⁷⁸ S. Dasu,⁷⁸ K. T. Flood,⁷⁸ J. J. Hollar,⁷⁸ P. E. Kutter,⁷⁸ Y. Pan,⁷⁸ M. Pierini,⁷⁸ R. Prepost,⁷⁸ S. L. Wu,⁷⁸ and H. Neal⁷⁹

(BABAR Collaboration)

¹Laboratoire de Physique des Particules, IN2P3/CNRS et Université de Savoie, F-74941 Annecy-Le-Vieux, France

²Universitat de Barcelona, Facultat de Física, Departament ECM, E-08028 Barcelona, Spain

³Università di Bari, Dipartimento di Fisica and INFN, I-70126 Bari, Italy

⁴University of Bergen, Institute of Physics, N-5007 Bergen, Norway

⁵Lawrence Berkeley National Laboratory and University of California, Berkeley, California 94720, USA

⁶University of Birmingham, Birmingham, B15 2TT, United Kingdom

⁷Ruhr Universität Bochum, Institut für Experimentalphysik 1, D-44780 Bochum, Germany

⁸University of Bristol, Bristol BS8 1TL, United Kingdom

⁹University of British Columbia, Vancouver, British Columbia, Canada V6T 1Z1

¹⁰Brunel University, Uxbridge, Middlesex UB8 3PH, United Kingdom

¹¹Budker Institute of Nuclear Physics, Novosibirsk 630090, Russia

¹²University of California at Irvine, Irvine, California 92697, USA

¹³University of California at Los Angeles, Los Angeles, California 90024, USA

¹⁴University of California at Riverside, Riverside, California 92521, USA

¹⁵University of California at San Diego, La Jolla, California 92093, USA

¹⁶University of California at Santa Barbara, Santa Barbara, California 93106, USA

¹⁷University of California at Santa Cruz, Institute for Particle Physics, Santa Cruz, California 95064, USA

¹⁸California Institute of Technology, Pasadena, California 91125, USA

¹⁹University of Cincinnati, Cincinnati, Ohio 45221, USA

²⁰University of Colorado, Boulder, Colorado 80309, USA

²¹Colorado State University, Fort Collins, Colorado 80523, USA

²²Universität Dortmund, Institut für Physik, D-44221 Dortmund, Germany

²³Technische Universität Dresden, Institut für Kern- und Teilchenphysik, D-01062 Dresden, Germany

²⁴Laboratoire Leprince-Ringuet, CNRS/IN2P3, Ecole Polytechnique, F-91128 Palaiseau, France

²⁵University of Edinburgh, Edinburgh EH9 3JZ, United Kingdom

²⁶Università di Ferrara, Dipartimento di Fisica and INFN, I-44100 Ferrara, Italy

²⁷Laboratori Nazionali di Frascati dell'INFN, I-00044 Frascati, Italy

²⁸Università di Genova, Dipartimento di Fisica and INFN, I-16146 Genova, Italy

²⁹Harvard University, Cambridge, Massachusetts 02138, USA

³⁰Universität Heidelberg, Physikalisches Institut, Philosophenweg 12, D-69120 Heidelberg, Germany

- ³¹Imperial College London, London, SW7 2AZ, United Kingdom
³²University of Iowa, Iowa City, Iowa 52242, USA
³³Iowa State University, Ames, Iowa 50011-3160, USA
³⁴Johns Hopkins University, Baltimore, Maryland 21218, USA
³⁵Universität Karlsruhe, Institut für Experimentelle Kernphysik, D-76021 Karlsruhe, Germany
³⁶Laboratoire de l'Accélérateur Linéaire, IN2P3/CNRS et Université Paris-Sud 11, Centre Scientifique d'Orsay, B. P. 34, F-91898 ORSAY Cedex, France
³⁷Lawrence Livermore National Laboratory, Livermore, California 94550, USA
³⁸University of Liverpool, Liverpool L69 7ZE, United Kingdom
³⁹Queen Mary, University of London, E1 4NS, United Kingdom
⁴⁰University of London, Royal Holloway and Bedford New College, Egham, Surrey TW20 0EX, United Kingdom
⁴¹University of Louisville, Louisville, Kentucky 40292, USA
⁴²University of Manchester, Manchester M13 9PL, United Kingdom
⁴³University of Maryland, College Park, Maryland 20742, USA
⁴⁴University of Massachusetts, Amherst, Massachusetts 01003, USA
⁴⁵Massachusetts Institute of Technology, Laboratory for Nuclear Science, Cambridge, Massachusetts 02139, USA
⁴⁶McGill University, Montréal, Québec, Canada H3A 2T8
⁴⁷Università di Milano, Dipartimento di Fisica and INFN, I-20133 Milano, Italy
⁴⁸University of Mississippi, University, Mississippi 38677, USA
⁴⁹Université de Montréal, Physique des Particules, Montréal, Québec, Canada H3C 3J7
⁵⁰Mount Holyoke College, South Hadley, Massachusetts 01075, USA
⁵¹Università di Napoli Federico II, Dipartimento di Scienze Fisiche and INFN, I-80126, Napoli, Italy
⁵²NIKHEF, National Institute for Nuclear Physics and High Energy Physics, NL-1009 DB Amsterdam, The Netherlands
⁵³University of Notre Dame, Notre Dame, Indiana 46556, USA
⁵⁴Ohio State University, Columbus, Ohio 43210, USA
⁵⁵University of Oregon, Eugene, Oregon 97403, USA
⁵⁶Università di Padova, Dipartimento di Fisica and INFN, I-35131 Padova, Italy
⁵⁷Laboratoire de Physique Nucléaire et de Hautes Energies, IN2P3/CNRS, Université Pierre et Marie Curie-Paris6, Université Denis Diderot-Paris7, F-75252 Paris, France
⁵⁸University of Pennsylvania, Philadelphia, Pennsylvania 19104, USA
⁵⁹Università di Perugia, Dipartimento di Fisica and INFN, I-06100 Perugia, Italy
⁶⁰Università di Pisa, Dipartimento di Fisica, Scuola Normale Superiore and INFN, I-56127 Pisa, Italy
⁶¹Princeton University, Princeton, New Jersey 08544, USA
⁶²Università di Roma La Sapienza, Dipartimento di Fisica and INFN, I-00185 Roma, Italy
⁶³Universität Rostock, D-18051 Rostock, Germany
⁶⁴Rutherford Appleton Laboratory, Chilton, Didcot, Oxon, OX11 0QX, United Kingdom
⁶⁵DSM/Dapnia, CEA/Saclay, F-91191 Gif-sur-Yvette, France
⁶⁶University of South Carolina, Columbia, South Carolina 29208, USA
⁶⁷Stanford Linear Accelerator Center, Stanford, California 94309, USA
⁶⁸Stanford University, Stanford, California 94305-4060, USA
⁶⁹State University of New York, Albany, New York 12222, USA
⁷⁰University of Tennessee, Knoxville, Tennessee 37996, USA
⁷¹University of Texas at Austin, Austin, Texas 78712, USA
⁷²University of Texas at Dallas, Richardson, Texas 75083, USA
⁷³Università di Torino, Dipartimento di Fisica Sperimentale and INFN, I-10125 Torino, Italy
⁷⁴Università di Trieste, Dipartimento di Fisica and INFN, I-34127 Trieste, Italy
⁷⁵IFIC, Universitat de Valencia-CSIC, E-46071 Valencia, Spain
⁷⁶University of Victoria, Victoria, British Columbia, Canada V8W 3P6
⁷⁷Department of Physics, University of Warwick, Coventry CV4 7AL, United Kingdom
⁷⁸University of Wisconsin, Madison, Wisconsin 53706, USA
⁷⁹Yale University, New Haven, Connecticut 06511, USA

(Received 27 August 2007; published 19 December 2007)

A search for the neutrinoless, lepton-flavor violating decay of the tau lepton into three charged leptons has been performed using 376 fb^{-1} of data collected at an e^+e^- center-of-mass energy around 10.58 GeV with the BABAR detector at the SLAC PEP-II storage rings. In all six decay modes considered, the numbers of events found in data are compatible with the background expectations. Upper limits on the branching fractions are set in the range $(4-8) \times 10^{-8}$ at 90% confidence level.

Lepton-flavor violation (LFV) involving charged leptons has never been observed, and stringent experimental limits exist from muon branching fractions: $\mathcal{B}(\mu \rightarrow e\gamma) < 1.2 \times 10^{-11}$ [1] and $\mathcal{B}(\mu \rightarrow eee) < 1.0 \times 10^{-12}$ [2] at 90% confidence level (C.L.). Recent results from neutrino oscillation experiments [3] show that LFV does indeed occur, although the branching fractions expected in charged lepton decays due to neutrino mixing alone are probably no more than 10^{-14} [4].

In tau decays, the most stringent limit on LFV is $\mathcal{B}(\tau \rightarrow \mu\gamma) < 4.5 \times 10^{-8}$ at 90% C.L. [5]. Many descriptions of physics beyond the standard model (SM), particularly models seeking to describe neutrino mixing, predict enhanced LFV in tau decays over muon decays with branching fractions from 10^{-10} up to the current experimental limits [6–8]. An observation of LFV in tau decays would be a clear signature of non-SM physics, while improved limits will provide further constraints on theoretical models.

This Letter presents a search for LFV in the neutrinoless decay $\tau^- \rightarrow \ell^- \ell^+ \ell^-$, where ℓ is an electron or muon. All possible lepton combinations consistent with charge conservation are considered, leading to six distinct decay modes ($e^- e^+ e^-$, $\mu^+ e^- e^-$, $\mu^- e^+ e^-$, $e^+ \mu^- \mu^-$, $e^- \mu^+ \mu^-$, $\mu^- \mu^+ \mu^-$) [9]. The analysis is based on data recorded by the *BABAR* detector at the PEP-II asymmetric-energy $e^+ e^-$ storage rings operated at the Stanford Linear Accelerator Center. The data sample consists of 339 fb^{-1} recorded at $\sqrt{s} = 10.58 \text{ GeV}$, and 37 fb^{-1} recorded at $\sqrt{s} = 10.54 \text{ GeV}$. With an expected cross section for tau pairs at the luminosity-weighted \sqrt{s} of $\sigma_{\tau\tau} = 0.919 \pm 0.003 \text{ nb}$ [10], this data sample contains about 690×10^6 tau decays.

The *BABAR* detector is described in detail in Ref. [11]. Charged-particle (track) momenta are measured with a 5-layer double-sided silicon vertex tracker and a 40-layer helium-isobutane drift chamber inside a 1.5-T superconducting solenoidal magnet. The transverse momentum resolution is parameterized as $\sigma_{p_T}/p_T = (0.13_{p_T}/[\text{GeV}/c] + 0.45)\%$. An electromagnetic calorimeter consisting of 6580 CsI(Tl) crystals is used to identify electrons and photons, a ring-imaging Cherenkov detector is used to identify charged hadrons, and the instrumented magnetic flux return (IFR), embedded with limited streamer tubes and resistive plate chambers, is used to identify muons.

A Monte Carlo (MC) simulation of lepton-flavor violating tau decays is used to optimize the parameter space for the search. Simulated tau-pair events including higher-order radiative corrections are generated using KK2F [12] with one tau decaying to three leptons with a three-body phase space distribution, while the other tau decays according to measured rates [13] simulated with TAUOLA [14]. Final-state radiative effects are simulated for all decays using PHOTOS [15]. The detector response is simulated with

GEANT4 [16], and the simulated events are then reconstructed in the same manner as the data.

The signature of the decay $\tau^- \rightarrow \ell^- \ell^+ \ell^-$ is a set of three charged particles, each identified as either an electron or muon, with an invariant mass and energy equal to that of the parent tau lepton. Candidate signal events in this analysis are required to have a “1–3 topology,” where one tau decay yields three charged particles, while the second tau decay yields one charged particle. Events with four well-reconstructed tracks and zero net charge are selected, and the tracks are required to point toward a common region consistent with $\tau^+ \tau^-$ production and decay. The polar angle of all four tracks in the laboratory frame is required to be within the calorimeter acceptance range. Pairs of oppositely charged tracks are ignored if their invariant mass, assuming electron mass hypotheses, is less than $30 \text{ MeV}/c^2$, as these tracks are likely to be from photon conversions in the traversed material. The event is divided into hemispheres in the $e^+ e^-$ center-of-mass (c.m.) frame using the plane perpendicular to the thrust axis, as calculated from the observed tracks and neutral energy deposits. The signal hemisphere must contain exactly three tracks while the other hemisphere must contain exactly one.

Each of the charged particles found in the signal hemisphere must be identified as either an electron or muon candidate. Electrons are identified using the ratio of calorimeter energy to track momentum (E/p), the ionization loss in the tracking system (dE/dx), and the shape of the shower in the calorimeter. Muon identification makes use of a neural net, inputs to which include the number of hits in the IFR, the number of interaction lengths traversed, and the energy deposition in the calorimeter. Muons with momentum less than $500 \text{ MeV}/c$ do not penetrate far enough into the IFR to be identified. For the lepton momentum spectrum predicted by the signal MC calculation, the electron and muon identification requirements are found to have an average efficiency per lepton of 91% and 65%, respectively. The probability for a pion to be misidentified as an electron in three-prong tau decays is 2.7%, while the probability to be misidentified as a muon is 2.9%.

The particle identification (PID) requirements are not sufficient to suppress certain backgrounds, particularly those from light-quark pair production and higher-order radiative Bhabha and $\mu^+ \mu^-$ events that can have four leptons in the final state. To reduce these backgrounds, additional selection criteria are applied to the six different decay modes. For all decay modes, the momentum of the track in the 1-prong hemisphere is required to be less than $4.8 \text{ GeV}/c$ in the c.m. frame. For signal events, the missing momentum is given by the momentum of the neutrino(s) coming from the tau in the one-prong hemisphere. The invariant mass of that hemisphere is calculated from the total missing momentum and energy combined with the one-prong track four-momentum, assuming the most-likely mass hypothesis for that track. The mass of the

one-prong hemisphere is required to be consistent with or smaller than the tau mass for all decay modes. For the $e^-e^+e^-$ and $\mu^-e^+e^-$ decay modes, radiative Bhabha events are suppressed by rejecting events with pairs of oppositely-charged electron tracks in the three-prong hemisphere with invariant mass less than $250 \text{ MeV}/c^2$. For the $e^-e^+e^-$ and $e^-\mu^+\mu^-$ decay modes, the charged particle in the one-prong hemisphere is required to deposit energy in the calorimeter, and must not be identified as an electron, while for the $\mu^-e^+e^-$ and $\mu^-\mu^+\mu^-$ decay modes this track must not be identified as a muon. For the $e^-e^+e^-$ and $e^-\mu^+\mu^-$ decay modes, the net transverse momentum of the four tracks must be greater than $400 \text{ MeV}/c$, while for the $\mu^-e^+e^-$ mode it must be greater than $200 \text{ MeV}/c$. Events in all six decay modes are required to have no track in the three-prong hemisphere that is consistent with being a kaon.

To reduce backgrounds further, candidate signal events are required to have an invariant mass and total energy in the three-prong hemisphere consistent with a parent tau lepton. These quantities are calculated from the observed track momenta assuming lepton masses that correspond to the specific decay mode. The energy difference is defined as $\Delta E \equiv E_{\text{rec}}^* - E_{\text{beam}}^*$, where E_{rec}^* is the total energy of the tracks observed in the three-prong hemisphere and E_{beam}^* is the beam energy, with both quantities measured in the c.m. frame. The mass difference is defined as $\Delta M \equiv M_{\text{rec}} - m_\tau$ where M_{rec} is the reconstructed invariant mass of the three tracks and $m_\tau = 1.777 \text{ GeV}/c^2$ is the tau mass [13].

The signal distributions in the $(\Delta M, \Delta E)$ plane (see Fig. 1) are broadened by detector resolution and radiative effects. In all decay modes, the radiation of photons from the incoming e^+e^- particles and from the outgoing tau particles leads to a tail at low values of ΔE . Radiation from the final-state leptons, which is more likely for electrons than muons, produces a tail at low values of ΔM as well. Rectangular signal regions are defined separately for each decay mode. The signal region boundaries are chosen to provide the smallest expected upper limits on the branching fractions in the background-only hypothesis. These expected upper limits are estimated using only MC simulations and data control samples, not candidate signal events. For all six decay modes, the upper right corner of the signal region in the $(\Delta M, \Delta E)$ plane is fixed at $(20, 50)$, while the lower left corner is at $(-50, -200)$ for the $\mu^-e^+e^-$ and $e^-\mu^+\mu^-$ decay modes, $(-70, -200)$ for $e^-e^+e^-$, $(-100, -350)$ for $\mu^+e^-e^-$, $(-50, -200)$ for $e^+\mu^-\mu^-$, and $(-20, -200)$ for $\mu^-\mu^+\mu^-$. All values are given in units of $(\text{MeV}/c^2, \text{MeV})$. Figure 1 shows the observed data in the $(\Delta M, \Delta E)$ plane, along with the signal region boundaries and the expected signal distributions. To avoid bias, a blinded analysis procedure was followed with the number of data events in the signal region remaining unknown until the selection criteria were finalized and all cross checks were performed.

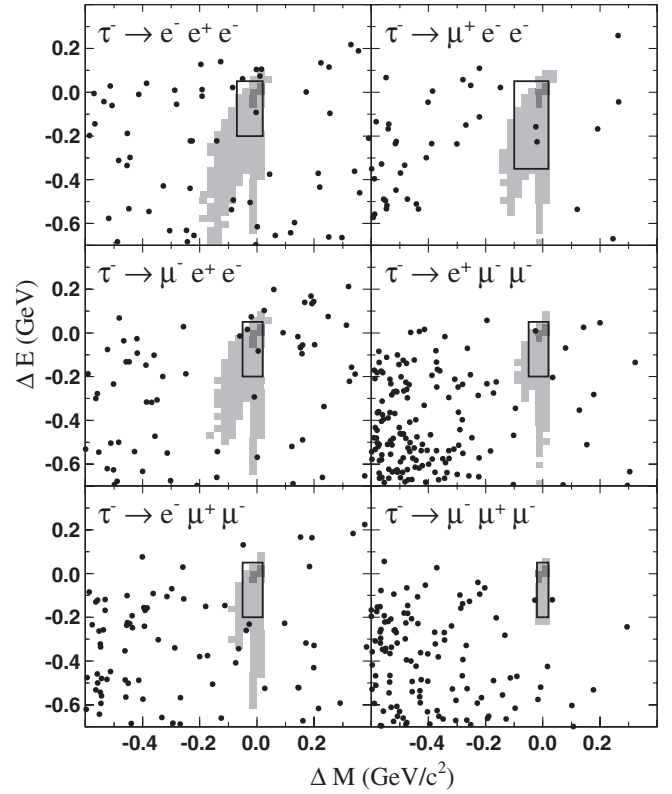


FIG. 1. Observed data shown as dots in the $(\Delta E, \Delta M)$ plane and the boundaries of the signal region for each decay mode. The dark and light shading indicates contours containing 50% and 90% of the selected MC signal events, respectively.

There are three main classes of background remaining after the selection criteria are applied: low multiplicity $q\bar{q}$ events (mainly continuum light-quark production); QED events (Bhabha and $\mu^+\mu^-$); and SM $\tau^+\tau^-$ events. These three background classes have distinctive distributions in the $(\Delta E, \Delta M)$ plane. The $q\bar{q}$ events tend to populate uniformly the region $\Delta E < 0.1 \text{ GeV}/c^2$ and exhibit a broad peak unrelated to m_τ in ΔM , while QED backgrounds are restricted to a narrow band at positive values of ΔE , and $\tau^+\tau^-$ backgrounds are restricted to negative values of both ΔE and ΔM . A negligible two-photon background remains.

The expected background rates for each decay mode are determined by fitting a set of probability density functions (PDFs) to the observed data in the grand sideband (GS) region of the $(\Delta E, \Delta M)$ plane. The GS region, shown in Fig. 1, lies between -600 and $400 \text{ MeV}/c^2$ in ΔM and -700 and 400 MeV in ΔE , excluding the signal region. For the $q\bar{q}$ background, a PDF is constructed from the product of two PDFs $P_{M'}$ and $P_{E'}$, where $P_{M'}(\Delta M')$ is a bifurcated Gaussian and $P_{E'}(\Delta E') = (1 - x/\sqrt{1+x^2}) \times (1 + ax + bx^2 + cx^3)$ with $x = (\Delta E' - d)/e$. The $(\Delta M', \Delta E')$ axes have been slightly rotated from $(\Delta M, \Delta E)$ to take into account the observed correlation between ΔE and ΔM for the distribution. The resulting PDF has a total of

eight fit parameters, including the rotation angle, all of which are determined by fits to MC $q\bar{q}$ background samples for each decay mode. For the $\tau^+\tau^-$ background PDF, the function $P_{M''}(\Delta M'')$ is the sum of two Gaussians with common mean, while the functional form of $P_{E''}(\Delta E'')$ is the same as that for the $q\bar{q}$ PDF. To properly model the wedge-shaped distribution due to the kinematic limit in tau decays, a coordinate transformation of the form $\Delta M'' = \cos \beta_1 \Delta M + \sin \beta_1 \Delta E$ and $\Delta E'' = \cos \beta_2 \Delta E - \sin \beta_2 \Delta M$ is performed. In total there are 11 free parameters describing this PDF, and all are determined by fits to the MC $\tau^+\tau^-$ samples.

For the three decay channels in which there is a significant QED background, an analytic PDF is constructed from the product of a Crystal Ball function [17] in $\Delta E'$ and a third-order polynomial in $\Delta M'$, where again the $(\Delta M', \Delta E')$ axes have been rotated slightly from $(\Delta E, \Delta M)$ to fit the observed distribution. The six parameters of this PDF, including the rotation angle, are obtained by fitting data control samples that are enhanced in Bhabha or $\mu^+\mu^-$ events.

With the shapes of the three background PDFs determined, an unbinned maximum likelihood fit to the data in the GS region is used to find the expected background rate in the signal region, shown in Table I. The PDF shape determinations and background fits are performed separately for each of the six decay modes.

The efficiency of the selection for signal events is estimated with a MC simulation of lepton-flavor violating tau decays. About 40% of the MC signal events pass the 1–3 topology requirement. The total efficiency for signal events to be found in the signal region is shown in Table I for each decay mode and ranges from 5.5% to 12.4%. This efficiency includes the 85% branching fraction for 1-prong tau decays.

The PID efficiencies and misidentification probabilities have been measured with control samples both for data and for MC events, as a function of particle momentum, polar angle, and azimuthal angle in the laboratory frame. The systematic uncertainties related to PID have been estimated from the statistical uncertainties of the efficiency

measurements and from their discrepancies between data and Monte Carlo calculation, and range from 2.3% for $e^-e^+e^-$ to 12.5% for $\mu^-\mu^+\mu^-$ [18]. The modeling of the tracking efficiency contributes an additional 1% uncertainty. All other sources of uncertainty in the signal efficiency are found to be small, including the statistical limitation of the MC signal samples, modeling in the generator of radiative effects, track momentum resolution, trigger performance, observables used in the selection criteria, and knowledge of the tau one-prong branching fractions. The signal efficiency has been estimated using a 3-body phase space model and no additional uncertainty is assigned for possible model dependence. Despite the effect of slow muons on the PID efficiency, the total selection efficiency is found to be uniform within 20% across 95% of the phase space for the three leptons.

Since the background levels are extracted directly from the data, systematic uncertainties on the background estimation are directly related to the background parameterization and the fit technique used. The finite data available in the GS region to determine the background rates contributes a significant uncertainty in all decay channels. Uncertainties related to the background PDFs are estimated by varying the background shape parameters within their errors and repeating the fits, and from changing the functional form of the PDFs. The total uncertainties on the background estimates are shown in Table I. Cross checks of the background estimation are performed by considering the number of events expected and observed in sideband regions immediately neighboring the signal region for each decay mode.

The numbers of events observed (N_{obs}) and the background expectations (N_{bgd}) are shown in Table I, with no significant excess found in any decay mode. Upper limits on the branching fractions are calculated according to $\mathcal{B}_{\text{UL}}^{90} = N_{\text{UL}}^{90} / (2\varepsilon \mathcal{L} \sigma_{\tau\tau})$, where N_{UL}^{90} is the 90% C.L. upper limit for the number of signal events when N_{obs} events are observed with N_{bgd} background events expected. The values ε , \mathcal{L} , and $\sigma_{\tau\tau}$ are the selection efficiency, luminosity, and $\tau^+\tau^-$ cross section, respectively. The uncertainty on the product $\mathcal{L}\sigma_{\tau\tau}$ is 1.0%. The branching fraction upper limits are calculated including all uncertainties using the technique of Cousins and Highland [19] following the implementation of Barlow [20]. The sensitivity or expected upper limit $\text{UL}_{90}^{\text{exp}}$, defined as the mean upper limit expected in the background-only hypothesis, is included in Table I. The 90% C.L. upper limits on the $\tau^- \rightarrow \ell^- \ell^+ \ell^-$ branching fractions are in the range $(4\text{--}8) \times 10^{-8}$. These limits represent up to an order of magnitude improvement over the previous experimental bounds [21,22].

We are grateful for the excellent luminosity and machine conditions provided by our PEP-II colleagues, and for the substantial dedicated effort from the computing organizations that support *BABAR*. The collaborating institutions wish to thank SLAC for its support and kind hospitality.

TABLE I. Efficiency estimates, number of expected background events (N_{bgd}), expected branching fraction upper limits at 90% C.L. ($\text{UL}_{90}^{\text{exp}}$), number of observed events (N_{obs}), and observed branching fraction upper limits at 90% C.L. ($\text{UL}_{90}^{\text{obs}}$) for each decay mode. All upper limits are in units of 10^{-8} .

Mode	Eff. [%]	N_{bgd}	$\text{UL}_{90}^{\text{exp}}$	N_{obs}	$\text{UL}_{90}^{\text{obs}}$
$e^-e^+e^-$	8.9 ± 0.2	1.33 ± 0.25	4.9	1	4.3
$\mu^-e^+e^-$	8.3 ± 0.6	0.89 ± 0.27	5.0	2	8.0
$\mu^+e^-e^-$	12.4 ± 0.8	0.30 ± 0.55	2.7	2	5.8
$e^+\mu^-\mu^-$	8.8 ± 0.8	0.54 ± 0.21	4.6	1	5.6
$e^-\mu^+\mu^-$	6.2 ± 0.5	0.81 ± 0.31	6.6	0	3.7
$\mu^-\mu^+\mu^-$	5.5 ± 0.7	0.33 ± 0.19	6.7	0	5.3

This work is supported by DOE and NSF (USA), NSERC (Canada), CEA and CNRS-IN2P3 (France), BMBF and DFG (Germany), INFN (Italy), FOM (The Netherlands), NFR (Norway), MIST (Russia), MEC (Spain), and STFC (United Kingdom). Individuals have received support from the Marie Curie EIF (European Union) and the A. P. Sloan Foundation.

*Deceased.

†Present address: Tel Aviv University, Tel Aviv, 69978, Israel.

‡Also with Università di Perugia, Dipartimento di Fisica, Perugia, Italy.

§Also with Università della Basilicata, Potenza, Italy.

||Also with Universitat de Barcelona, Facultat de Física, Departament ECM, E-08028 Barcelona, Spain.

- [1] M. L. Brooks *et al.* (MEGA/LAMPF Collaboration), Phys. Rev. Lett. **83**, 1521 (1999).
- [2] U. Bellgardt *et al.* (SINDRUM Collaboration), Nucl. Phys. B **299**, 1 (1988).
- [3] M. H. Ahn *et al.* (K2K Collaboration), Phys. Rev. Lett. **90**, 041801 (2003); K. Eguchi *et al.* (KamLAND Collaboration), Phys. Rev. Lett. **90**, 021802 (2003); Q. R. Ahmad *et al.* (SNO Collaboration), Phys. Rev. Lett. **89**, 011301 (2002); Y. Fukuda *et al.* (Super-Kamiokande Collaboration), Phys. Rev. Lett. **81**, 1562 (1998).
- [4] X. Y. Pham, Eur. Phys. J. C **8**, 513 (1999).
- [5] K. Hayasaka *et al.* (Belle Collaboration), arXiv:0705.0650.
- [6] P. Paradisi, J. High Energy Phys. **10** (2005) 006.
- [7] K. S. Babu and C. Kolda, Phys. Rev. Lett. **89**, 241802 (2002).
- [8] A. Brignole and A. Rossi, Phys. Lett. B **566**, 217 (2003).
- [9] Throughout this Letter, charge conjugate decay modes also are implied.
- [10] S. Banerjee, B. Pietrzyk, J. M. Roney, and Z. Wäs, arXiv:0706.3235.
- [11] B. Aubert *et al.* (BABAR Collaboration), Nucl. Instrum. Methods Phys. Res., Sect. A **479**, 1 (2002).
- [12] B. F. Ward, S. Jadach, and Z. Wäs, Nucl. Phys. B, Proc. Suppl. **116**, 73 (2003).
- [13] Y.-M. Yao *et al.* (Particle Data Group), J. Phys. G **33**, 1 (2006).
- [14] S. Jadach, Z. Wäs, R. Decker, and J. H. Kühn, Comput. Phys. Commun. **76**, 361 (1993).
- [15] E. Barberio and Z. Wäs, Comput. Phys. Commun. **79**, 291 (1994).
- [16] S. Agostinelli *et al.* (GEANT4 Collaboration), Nucl. Instrum. Methods Phys. Res., Sect. A **506**, 250 (2003).
- [17] M. J. Oreglia, Ph.D. thesis, SLAC-236, 1980, Appendix D; J. E. Gaiser, Ph.D. thesis, SLAC-255, 1982, Appendix F; T. Skwarnicki, Ph.D. thesis, DESY F31-86-02, 1986, Appendix E.
- [18] All uncertainties quoted in the text are relative.
- [19] R. D. Cousins and V. L. Highland, Nucl. Instrum. Methods Phys. Res., Sect. A **320**, 331 (1992).
- [20] R. Barlow, Comput. Phys. Commun. **149**, 97 (2002).
- [21] B. Aubert *et al.* (BABAR Collaboration), Phys. Rev. Lett. **92**, 121801 (2004).
- [22] Y. Yusa *et al.* (Belle Collaboration), Phys. Lett. B **589**, 103 (2004).